High Performance Materials Based on a Self-Assembled Multiple-Percolated Ternary Blend

Sepehr Ravati, Christine Beaulieu, Ali M. Zolali, and Basil D. Favis
CREPEC, Dept. of Chemical Engineering, École Polytechnique de Montréal, Montréal, QC H3C3A7, Canada

DOI 10.1002/aic.14495
Published online June 2, 2014 in Wiley Online Library (wileyonlinelibrary.com)

In this study, it will be shown that morphologically tailored tricontinuous ternary blends, comprising polybutylene succinate (PBS), polylactic acid (PLA), and poly (butylene adipate-co-terephthalate)(PBAT), can generate new materials with excellent properties. Detailed morphological analysis is used to establish that all three phases in the ternary 33%PBS/33%PLA/33%PBAT blend morphology are highly continuous with a phase structure dominated by complete wetting dynamics. PBS is shown to situate itself between PLA and PBAT. This melt processed, self-assembled, multiple percolated, blend possesses a high elongation at break (567%), high Young's modulus (1130 MPa), high impact strength (271 J/m), and a storage modulus about 50% higher than pure PBS at room temperature. None of the neat materials demonstrate this combination of high properties and the synergy derives from the tricontinuous structure of the system. The ternary nature of the blend allows for a modulation of the crystallinity behavior as examined by differential scanning calorimeter and X-ray Diffraction. © 2014 American Institute of Chemical Engineers *AIChE J*, 60: 3005–3012, 2014
Keywords: double-percolated, ternary polymer blend, morphology, mechanical properties, poly (butylene succinate), poly (lactic acid), poly (butylene adipate-co-terephthalate)

Introduction

Biopolymers have potential as sustainable replacements to traditional petroleum-based materials if innovative methods are used to improve their properties. The main advantage of such polymers is their low environmental footprint if they can be properly recycled or composted.[1] During the past decade, polybutylene succinate (PBS) has attracted considerable attention as a promising biodegradable aliphatic polyester. This polymer, depending on its degree of crystallinity, can show different levels of flexibility and toughness.[2,3] PBS has many desirable properties such as melt-processability, thermal and chemical resistance, and good toughness, although crystalline grades of PBS show lower levels of flexibility[4] due to a low storage modulus and relatively low Young's modulus at room temperature. Polylactic acid (PLA) and poly (butylene adipate-co-terephthalate) (PBAT) are two important raw materials for many compostable and bio-based polymer blends. PLA is a linear, bio-based and aliphatic polyester produced via bacterial fermentation. PBAT is classified as a biodegradable aliphatic-aromatic copolyester.[5]

A high performance material requires high levels of ductility, stiffness, and strength. Generally, designing materials having both high stiffness and high toughness (a balance of strength and ductility) is difficult to achieve. For example, PLA exhibits high modulus with low impact resistance. Conversely, PBAT is a high strain-to-failure material showing poor stiffness. This competition between the elastic and plastic deformation of polymers mechanical behavior can be overcome by tuning the mechanical properties through melt-blending the components and controlling the morphology.[6]

Many different types of morphologies can be obtained for multicomponent polymer blends that directly affect the whole set of properties.[7–9] A ternary polymer blend system can show a variety of complex structures including both complete wetting and partial wetting phenomena.[10,11] In the complete wetting case, one of the most complex morphologies is a tricontinuous system where a continuous polymer (A) is situated at the interface of a cocontinuous B/C system.[12] In this tricontinuous morphology, all phases are highly continuous and percolated throughout the blend.[10] The origin of this interfacial tension driven, multiple-percolated structure can be understood from spreading coefficient theory.[13,14] Harkins spreading theory predicts a complete wetting morphology in a ternary blend when one of the spreading coefficients calculated by Eq. 1 has a positive value

$$\lambda_{AB} = \gamma_{BC} - \gamma_{AC} - \gamma_{AB} \tag{1}$$

where γ represents the interfacial tensions for the different polymer pairs and subindices refer to each component in the mixture. λ is the spreading coefficient giving the tendency of one component to spread over another component. A positive value for λ_{AB}, determines that phase (A) separates phases (B) and (C) indicating a complete wetting morphology (two-phase contact only). Negative values for all spreading coefficients in a ternary polymer blend indicate a partial wetting morphology where droplets of one of the phases situate at the interface and demonstrate a three-phase contact.

Correspondence concerning this article should be addressed to B. D. Favis at basil.favis@polymtl.ca.

Table 1. Material Characteristics and Thermal Properties

Material	$\eta \times 10^{-3}$ at 25 s^{-1} (Pa s)[a]	ρ (g/cm^3) at 200°C	T_{mPeak} (°C)[b]	T_{ccPeak} (°C)[c]	ΔH_m (J/g)[d]	ΔH_{rc} (J/g)[e]	$\Delta H_{100\%c}$ (J/g)[f]	(%) Crystallinity
PLA	1.01	1.12	169.2	134	15.1	15.1	93.7	0%
PBS	0.41	1.1	116.2	99	55	5.9	110.3	44.5%
PBAT	0.9	1.1	123	–	13.3	–	114	11.7%

[a]Viscosity measured at 180°C.
[b]Melt peak temperature.
[c]Cold-crystallization temperature.
[d]Enthalpy of fusion.
[e]Enthalpy of cold-crystallization.
[f]Enthalpy of fusion of 100% crystalline polymer.

The mechanical properties of a multicomponent blend are considerably affected by the crystallinity of the components. Typically, increased levels of crystallization in a polymer result in a decrease in the fracture toughness and increase the embrittlement of the material.[15,16] The toughness and strength of semicrystalline systems are interdependent and both are dependent on cavitation and plastic deformation of crystalline and amorphous phases.[17] The polymer crystallization process always accompanies a decrease in specific volume that results in the creation of cavitation bubbles. Such cavitation bubbles are known as "weak spots" and propagate at interspherulitic regions, resulting in the decrease of mechanical properties of polymer materials.[18] A lower mid-level of crystallinity, however, results in an enhancement of toughness and material strength, as well as the formation of a considerable amount of cavitation.[19]

The objective of this study is to examine the potential of tailoring the properties in a PBS, PLA, and PBAT system through the preparation of a tricontinuous polymer blend. The morphology, continuity, mechanical properties and crystallinity of the system will be evaluated.

Experimental Methods

Materials

Commercial homopolymers of PBS (Mitsubishi Chemical), PLA (Natureworks, 3001D), and PBAT (BASF Ecoflex) were all used as received. The properties are listed in a previous article from this lab.[20] The main characteristics of the materials used are listed in Table 1.

Sample preparation

Binary and ternary blends were prepared via melt-blending under a flow of dry nitrogen in a 30 mL Brabender operating at a set temperature of 190°C and 50 rpm. The maximum shear rate at this speed is close to 25 s^{-1}. The mixing chamber was filled to 70% of its total volume. A concentration of 0.2 weight percent of Irganox antioxidant supplied by CIBA was added to the mixture. All the blends were mixed for 8 min at which the torque achieves a constant plateau value. After mixing, the samples were immediately cut from the mass and quenched in a cold water bath to freeze-in the morphology.

Rheological analysis

The disc-shaped samples were compression molded in the hot press at 185°C. An AR2000 Rheometer from TA Instruments in the dynamic mode equipped with 25 mm parallel disk geometry was utilized to measure the linear viscoelastic properties of homopolymers containing 0.2% antioxidant. All homopolymers used here are known to follow the Cox–Merz equation,[21] consequently, the applied frequency can be considered as the shear rate and the complex viscosity as the steady shear viscosity. All polymers were found to be stable at the set temperature in the time sweep test for 8 min. After the determination of the viscoelastic region by stress sweep from 10 to 10,000 Pa, a frequency sweep allowed for the measure of the zero shear viscosity of each sample (Figure 1). The average shear rate in the mixer is approximately 25 s^{-1}. The viscosities at 25 s^{-1} for the various homopolymers are reported in Table 1.

Solvent extraction

A solvent extraction/gravimetric method was used to obtain quantitative data on the extent of continuity of the phases. Dichloroethane (DCE) was used to extract all phases except PBS at room temperature. As a primary advantage, solvent extraction is an absolute measurement and is also a straightforward technique to detect the existence of cocontinuous microstructures when the components are soluble in specific solvents.

$$\%\,\text{Continuity} = \frac{\sum_n V_{\text{initial}} - \sum_n V_{\text{final}}}{\sum_n V_{\text{initial}}} \times 100 \qquad (2)$$

Where V_{initial} and V_{final} are the volume of one component present in the sample before and after extraction calculated by weighing the sample and converting it to the volume. The degree of continuity represents the fraction of a phase that is continuous. Samples in which each phase has a degree of continuity of 1.0 are completely continuous. The reported value is the average of several samples and the average error for high continuity levels is ±5%.

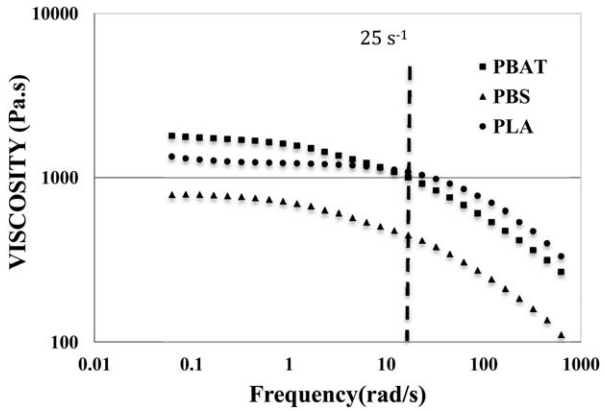

Figure 1. Complex viscosity vs. frequency for PBAT■, PBS▲, and PLA•.

Dynamic mechanic thermal analysis

A TA dynamic mechanical analyzer (*DMA 2980* from TA instruments) was used to measure dynamic thermal properties of the samples. A heating rate of 2°C/min was selected. The temperature range was selected according to the glass transition and melting temperatures of the components and was examined over a wide range of −100 to 100°C. A dual cantilever clamp mode on injection molded samples of size $126.4 \times 12.5 \times 3.1$ mm^3 was used.

Differential scanning calorimeter

A TA differential scanning calorimeter (*DSC Q1000*) was used to analyze the thermal behavior of the samples. After calibration of the temperature and enthalpy parameters with indium ($T_m = 156.6$°C, $\Delta H = 28.45$ J/g), the samples were weighed and sealed in a standard pan. A heating rate of 15°C/min was used and the glass transition temperature and melting temperature of the samples were evaluated.

The degree of crystallinity in a material can be calculated via DSC by the following equation

$$\%\,\text{Crystallinity} = \frac{(\Delta H_m - \Delta H_C)}{\Delta H_{\text{lit}}} \times 100 \tag{3}$$

Where ΔH_m represents enthalpy of fusion, ΔH_C is enthalpy of cold-crystallization and ΔH_{lit} represents enthalpy of melting for 100% crystalline material.

Tensile measurement

According to *ASTM D638*, tensile strength measurements were performed on an *Instron 3365* tensile testing apparatus. Testing was carried out with a tensile tester equipped with a 5 kN load cell and a crosshead speed of 5 mm/min. Samples were conditioned for 24 h at 22°C and 50% humidity. An average and standard deviation based on at least seven samples were reported.

Notched impact strength

Impact testing was carried out with an Izod impact pendulum, model *CS-137C-176*, from the CSI Company. Rectangular bars of samples with dimensions of 6 cm × 1.3 cm × 3.1 mm were injected molded with a Sumitomo SE50S injection machine. Samples were conditioned for 24 h at 22°C and 50% humidity. The samples were notched according to the *ASTM D256* standard. The sample was vertically inserted inside the equipment where the notch faces the impact pendulum. For each sample six notched specimens were tested and their average value and standard deviation were reported.

Microtoming, selective extraction, and scanning electron microscopy

The specimens were cut and microtomed to a plane face under liquid nitrogen using a microtome (Leica-Jung RM 2065) equipped with a glass knife and a cryochamber type (LN 21). After the appropriate chemical treatment at room temperature with selective solvents (acetic acid for differentiation of phases and DCE for all polymers except PBS) to remove one or several components, the sample surface was coated with gold/palladium by plasma deposition. A field emission gun scanning electron microscope (FEG-SEM) operated at a voltage of 2 to 5 keV, was used to obtain photomicrographs of the sample surface.

Morphological characterization of phases by optical microscopy and DSC

Thin layers of samples about 30 μm in thickness were used for the annealing process using a Mettler FP-82HT hot stage controlled with a Mettler FP-90 central processor. Photomicrographs were taken by a Nikon $F601_M$ camera connected to a Nikon transmission light microscope. Samples were heated from 25 to 200°C and then cooled down to room temperature. The polarized lens detects the crystalline structure of the various phases. The DSC curve allows to establish the crystalline temperature of each component.

Field emission gun scanning electron microscopy and atomic force microscopy

For FEG-SEM, a microtomed surface of the sample was treated with DCE or tetrahydrofuran (THF) at room temperature to selectively etch out a component. This was then coated with a gold/palladium alloy using plasma deposition. The field emission gun scanning electron microscope, operated at a voltage of 2 keV, was used to obtain photomicrographs of the sample surface. The extracted surface of the specimens was also examined by scanning probe microscope dimension atomic force microscopy (AFM) with a Nanoscope IIIa controller in tapping mode. The atomic force microscope measured topography with a force probe.

Results and Discussion

For a binary blend, the morphological system in which both components can best contribute to the final properties is a cocontinuous structure due to the percolation of all phases.[16,22] A few studies on such systems have reported considerable morphology-induced variations on mechanical properties.[22–24] In matrix-droplet structures the properties are still typically dominated by the matrix polymer.[23] In this study, an immiscible ternary blend with three percolated phases is even more advantageous because the property sets obtained in the final mixture can potentially be shared from three different polymers. This provides the opportunity to tailor a high level of balanced properties. The continuity of the components in this case allows them to better contribute to the final mechanical properties of the blend as compared to other classes of morphologies, providing that interfaces show relatively strong adhesion. A multiple-percolated structure could also be advantageous from a biodegradation point of view due to its facilitation of the biodegradation process in the blend by increasing the surface area of each polymer. Although the T_g peaks of PBS and PBAT slightly overlap, the immiscibility of the ternary PBS/PLA/PBAT blend is confirmed by the DMA loss modulus (not shown here).

The Harkins spreading theory for the ternary PBS/PLA/PBAT blend shows a positive spreading coefficient of $\lambda_{\text{PBS/PBAT}}$ with a value of 0.31 ± 0.24 mN/m.[25] It predicts complete wetting with the PBAT phase located at the interface of PLA and PBS. Despite this prediction, the very low value of the spreading coefficient and the associated experimental error makes it difficult to be conclusive about the spreading behavior. Experimental observations of the location of phases will be discussed in more detail below. Figure 2 shows the morphology of the 33%PBS/33%PLA/33%PBAT blend, all phases are percolated and a tricontinuous microstructure is produced. This morphology confirms the immiscibility of the ternary blend as also observed by DMA

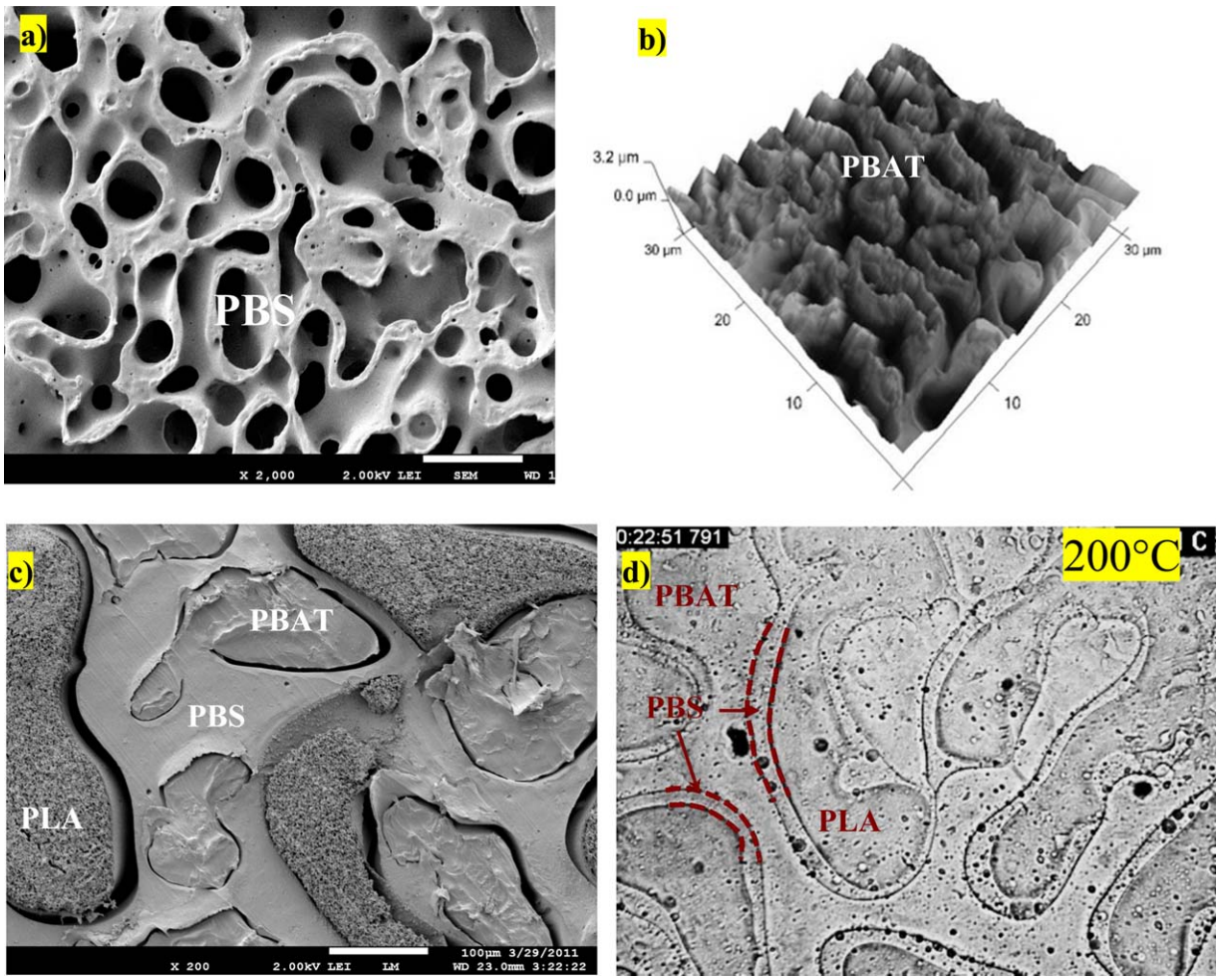

Figure 2. Ternary blend of 33%PBS/33%PLA/33%PBAT, a) SEM micrograph of PBS continuous structure after extraction of PLA and PBAT by DCE, b) AFM topographical image of PBAT continuous structure after treatment of sample surface by THF, c) SEM micrograph of sample after annealing and treatment with acetic acid, d) optical micrograph of sample after annealing at 200°C.

[Color figure can be viewed in the online issue, which is available at wileyonlinelibrary.com.]

analysis. Figure 2a shows the continuous PBS phase after extraction of both PLA and PBAT phases by DCE. In this case, gravimetric solvent extraction results reveal a $97 \pm 2\%$ continuity for PBS after extraction of the other phases. Figure 2b shows the continuous structure of the PBAT phase after treatment of the sample surface by THF. SEM (Figure 2c) and optical microscopy (Figure 2d) morphological analysis exhibit three percolated phases for the ternary polymer blend. In this work, the ternary blend of 33%PBS/33%PLA/33%PBAT was carefully selected to achieve a double percolated morphology as shown in Figure 2. Second, 33% of each phase allows for a balanced contribution of each component related to the properties of the blend. The components themselves, as mentioned earlier were carefully selected to demonstrate a maximum complementarity of base properties.

The samples in these figures were subjected to 30 min of annealing at 200°C to better visualize the morphology of the tricontinuous structure. As all the phases are polyesters with similar chemical structures, the morphological identification of phases is difficult due to the lack of a selective solvent for each phase. In previous work,[25] it was reported that the PBAT phase was situated between PBS and PLA. That conclusion was reached by considering the crystallization temperature of the materials as they cooled on the hot stage of the light microscope and then comparing that temperature to the crystallization temperatures of the neat materials. In continuing that work in this article, however, it was observed that in the ternary system each phase impacts the crystallinity of the other so that a comparison to the neat materials is not the correct approach as outlined below. Pure PBAT and PBS spherulites form at 52.3 and 78.4°C (Figures 3a, b). Such crystallization temperatures correspond to the DSC cooling run and crystalline peaks obtained for PBAT and PBS as shown in Figure 4. Figure 3c shows that for a binary blend of 50%PBS/50%PBAT both phases crystallize at 65.6°C indicating the role of the PBS phase as a nucleating agent for the PBAT phase. This temperature is higher than that for the crystallization of the PBAT phase as shown in Figure 3a. Once PBS crystallization commences at about 78.4°C at the interface, PBAT phase crystallization also begins by induction. As shown in Figure 3d, the ternary blend of 33%PBS/33%PLA/33%PBAT represents crystalline structures for PBAT and PBS phases at 56.9°C. In this case, the phases can be recognized by their crystallization temperature.

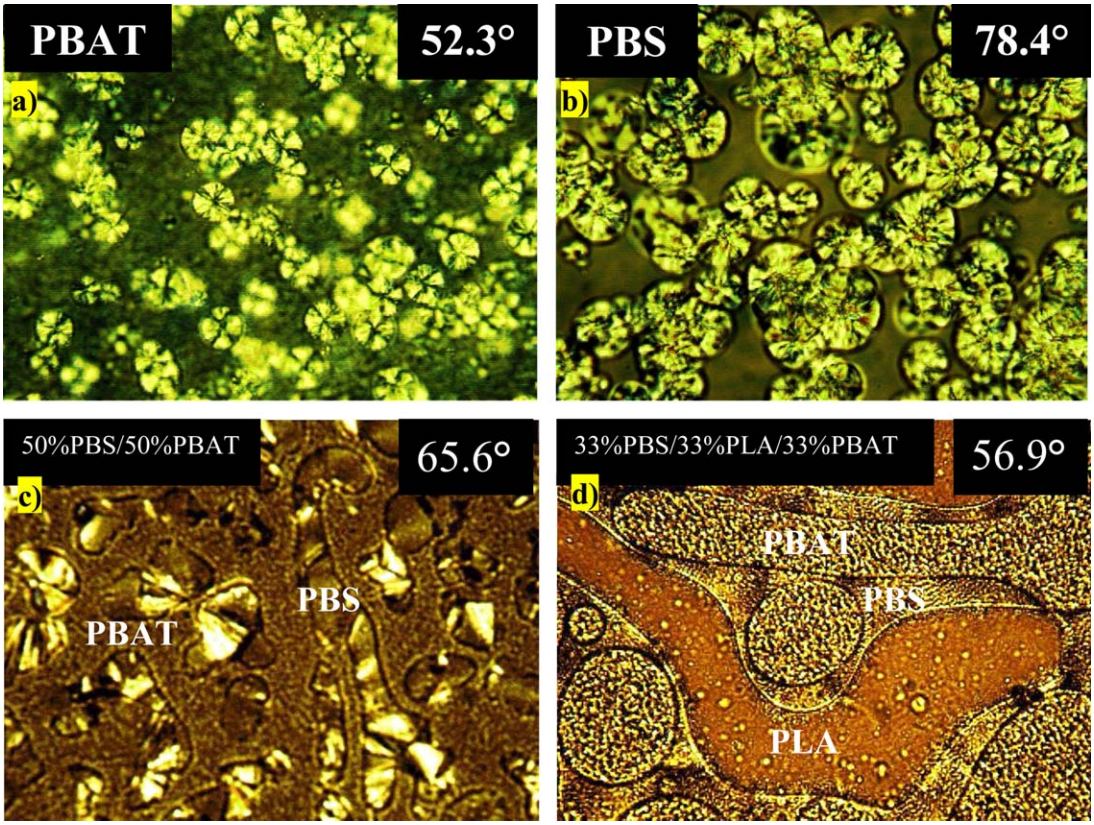

Figure 3. Crystalline structures of samples under polarized optical microscopy after cooling down the temperature to crystalline temperature of phases: a) spherulites of pure PBAT, b) spherulites of pure PBS, c) binary 50%PBS/50%PBAT blend after initiation of crystallization of both PBAT and PBS, and d) ternary 33%PBS/33%PLA/33%PBAT blend after initiating crystallization of all three phases.

[Color figure can be viewed in the online issue, which is available at wileyonlinelibrary.com.]

The second DSC cooling run for 33%PBS/33%PLA/33%PBAT shows that the crystalline behavior starts at 93°C (Figure 4). In this case, the crystallization of both the PBS and PBAT phases starts at higher temperature (93°C) indicating that PLA plays a major role as a nucleating agent. Figure 4 shows a single peak for the crystallization of the ternary blend confirming crystallization of all three phases together with a crystallization temperature higher than that of pure PBS and pure PBAT. Supplementary morphological images show that the crystalline structure of phases starts from the interface of the phases and that is in agreement with available theories.[26] Moreover, it is possible that the crystallinity is also affected by an interchange reaction between the polyesters. In an upcoming article, (Ravati et al., *Polymer*, Submitted) Time-of-Flight Secondary Ion Mass Spectrometry (ToF-SIMS) has been used to examine the interfacial transitions in similar polyester-based ternary blends. Very high resolution ToF-SIMS has been able to detect the formation of a new chemical species at the polyester-polyester interface. These appear to be due to transesterification. Based on these new data, the correct identification of phases in this ternary blend is represented in Figure 2 where the PBS phase locates between PBAT and PLA.

In this study, due to the existence of three polyesters with a high similarity in chemical structure, a relatively high interfacial adhesion at the interfaces is expected. This is confirmed by the very low interfacial tension values between phases as reported previously by Ravati and Favis.[25] Interfacial tensions were calculated using measured contact angles in the semiempirical Harmonic mean equation. Although estimating the interfacial tensions with such a semiempirical approach is less desirable than a fully experimental analysis, it should be noted that in this special case of very low interfacial tensions, it is the best and most reliable method to obtain interfacial tension data. Other methods such as the breaking thread technique were also tried, but due to the low interfacial tension values between polymer pairs, the thread of component (A) did not break in the matrix of component (B) even after 90 min.[25] In the Harmonic mean approach, the error from the contact angle measurements is

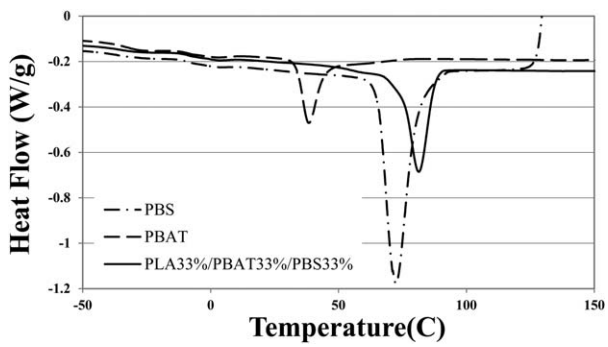

Figure 4. DSC thermograms for first cooling run of pure PBAT and PBS, and ternary 33%PBS/33%PLA/33%PBAT.

Table 2. Mechanical Properties of Pure Polymers and Polymer Blends

Name	Impact Strength (J/m)	Young's Modulus (Mpa)	Stress at Yield (MPa)	Elongation at Break (%)
PBS	58.7 ± 6.3	791.1 ± 43.3	40.4 ± 0.1	354.4 ± 37.4
PLA	23.2 ± 2.5	3331 ± 312.9	60 ± 0.4	7.6 ± 0.5
PBAT	>200	102.2 ± 5.4	–	>1000
PBS50%/PBAT50%	>200	258.3 ± 35.1	34.9 ± 0.9	>1000
PBS50%/PLA50%	34.5 ± 4.8	1721 ± 17	28.4 ± 0.5	56.2 ± 1.1
PBS33%/PLA33%/PBAT33%	271.3 ± 101.5	1130.9 ± 83.6	26.9 ± 0.1	567.9 ± 0.3

represented. Note that a high interfacial adhesion between the phases is critical to improve the final mechanical properties of the blend.

The mechanical properties are reported in Table 2 for both binary and ternary blends. The binary 50%PBS/50%PBAT blend, with cocontinuous morphology shows a significant improvement of ductility as compared to neat PBS, however, the modulus decreases significantly. Such properties are obtained due to a combination of PBAT ductility, the higher modulus of PBS, and the cocontinuity of both phases in the system. Conversely, a 50%PBS/50%PLA blend with a cocontinuous microstructure shows a very high modulus and lower EB compared to pure PBS. The ternary blend of 33%PBS/33%PLA/33%PBAT demonstrates a very high level of complementary properties, as shown in Table 2. The blend shows a high elongation at break (567%), high Young's modulus (1130 MPa) and high impact strength (271 J/m). None of the neat materials demonstrate this combination of high properties. These results indicate the mechanical property potential of a three-phase system where all components are fully percolated with high levels of interfacial interactions.

In a multicomponent polymer blend with a tricontinuous morphology, the modulus is expected to be determined by the concentration of the phases and the storage modulus of each component.[27,28] For the 33%PBS/33%PLA/33%PBAT ternary blend, it is shown in Figure 5a that the PBAT component reduces the storage modulus of PBS at both the low temperature range (−80 to −25°C) and high temperature range (−5 to 45°C). The presence of PLA, however, increases the PBS modulus by 50% at environmental temperatures (0 to 50°C). Figure 5b shows a magnified part of the DMA plot represented in Figure 5a. It can be seen that the storage modulus of PBS increases from 540 to 710 MPa for the ternary blend at 20°C.

Because the mechanical properties of polymer blends are greatly influenced by the crystallinity level of the blend, this second part of the work will examine the crystallinity behavior of the blend. An optimized toughness and tensile strength are strongly dependent on the level of crystallinity with semicrystalline structures generally preferred. In this study, highly crystalline PBS, semicrystalline PBAT and completely amorphous PLA are used. The DSC and wide-angle x-ray diffraction patterns (WAXD) are used to characterize the crystalline behavior of the polymers. For the pure samples, as shown in Table 1, the DSC reports 0% crystallinity for PLA, since the enthalpy values for cold-crystallization and fusion are equal at 15.1 J/g. Table 1 also reveals an 11.7% crystallinity for PBAT, because no cold crystallization peak appears and the enthalpy of melting for such a polymer is measured to have a value of 13.3 J/g. The enthalpy of melting[29] for 100% crystalline PBAT has a value of 114 J/g. PBS shows an exothermal cold-crystallization peak just before its endothermal melting peak at 116.2°C. The enthalpy of crystallization and melting enthalpy for PBS are 5.9 and 55 J/g, respectively. The polymer handbook reports an enthalpy of melting value of 110.3 J/g for 100% crystalline PBS. The percent crystallinity for the PBS used in this study can thus be estimated to be 44.5%.

In the previous part of the work, it was observed that in the ternary 33%PBS/33%PLA/33%PBAT blend, certain phases act as nucleating agents for other phases and shift the crystalline temperature of those phases. To obtain the total degree of crystallinity in such a blend, the second heating run of DSC thermograms scanned at 15°C/min as summarized in Figure 6 is used. It can be seen that the PBS and PLA phases cold-crystallize at 106°C and at about 135°C, respectively. For this ternary blend, the melting peak for PBAT disappears as the crystalline part of PBAT nucleates PBS at 115°C and the small peak for PBAT overlaps with the large PBS melting peak. The DSC experiments demonstrate that the crystallinity of the 33%PBS/33%PLA/33%PBAT blend has been modulated through the blending

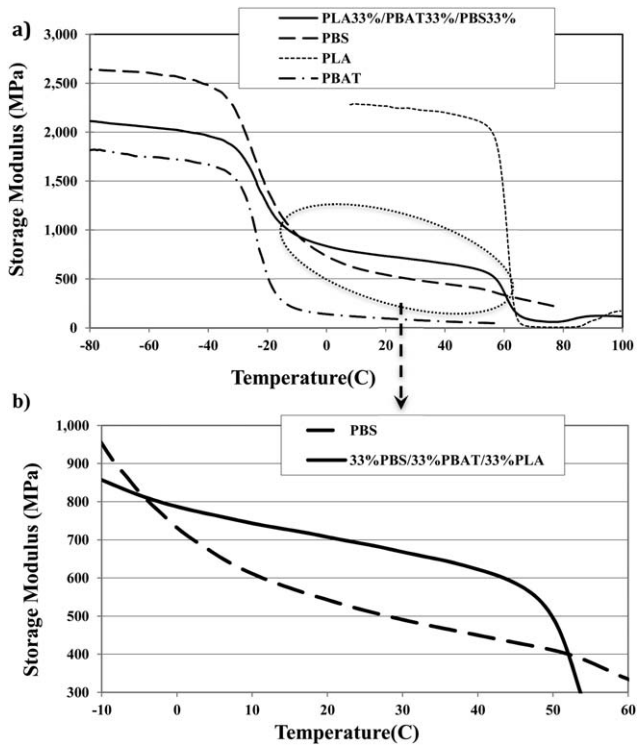

Figure 5. DMA thermograms for storage modulus vs. temperature of PBS, PLA, PBAT, and 33%PBS/33%PLA/33%PBAT, a) wide temperature range between −80 and 100°C, b) narrow temperature range between −10 and 60°C used for conventional applications.

process to a value of 17%. This lower percent crystallinity for the blend could also be due to transesterification because crystallinity in multicomponent blends starts at the interface. As mentioned earlier in this article an upcoming work using ToF-SIMS will be reporting on the formation of a new chemical species at the polyester-polyester interface.(Ravati et al., *Polymer*, Submitted) This is critical to achieve high elongation and high impact for the blend. Typical lower crystallinity can assist in the creation of cavitation in such systems resulting in dissipative processes, such as shear yielding and crazing.

The WAXD of the ternary 33%PBS/33%PLA/33%PBAT system confirms that the PBS and PBAT crystal structure remains constant after blending (Figure 7). The WAXD pattern for PBS in Figure 7a exhibits diffraction peaks located at $2\theta = 19.5$, 21.7, 22.6, and 28.6° corresponding to the (0 2 0), (0 2 1), and (1 1 0) planes of the α-form of the PBS crystal, respectively.[30] Ihn et al.[31] used electron diffraction patterns to demonstrate that the α-form crystal structure of PBS is monoclinic with unit cell dimensions $a = 0.523$ nm, $b = 0.908$ nm, $c = 1.079$ nm, and $\beta = 124°$, as well as with a T_7GTG conformation. A diffuse amorphous hump of large magnitude is obtained for the WAXD pattern of the PLA specimen. Other researchers have reported a similar diffraction pattern for amorphous PLA polymers.[32–34] Figure 7a also shows the WAXD pattern of the pure PBAT specimen, demonstrating insignificant diffraction peaks centered at $2\theta = 16$, 17.4, 23, and 24.6°. Such small diffraction peaks for PBAT correspond to the formation of small amounts of weak PBAT crystals.[34,35] Figure 7b shows diffraction peaks of the 33%PBS/33%PLA/33%PBAT blend, demonstrating no shift for the diffraction peaks of PBAT and PBS phases. This indicates that the crystalline structure for the PBAT and the PBS phases is maintained after blending.

Conclusions

In this study, the morphology and properties of a tricontinuous ternary PBS/PLA/PBAT immiscible blend is examined. The Harkins spreading theory for this ternary blend shows a positive spreading coefficient of $\lambda_{PBS/PBAT}$ with a value of 0.3 ± 0.2 mN/m. Although it predicts complete wetting with the PBAT phase located at the interface of PLA and PBS, morphological observations show the PBS phase at the interface. Morphological observations also show continuous PBAT and PBS phases after selective extraction with solvents. Moreover, gravimetric solvent extraction results reveal a $97 \pm 2\%$ continuity for PBS after extraction of the other phases. By compositional control of such a blend at 33%PBS/33%PLA/33%PBAT, all phases are percolated and a tricontinuous microstructure is produced.

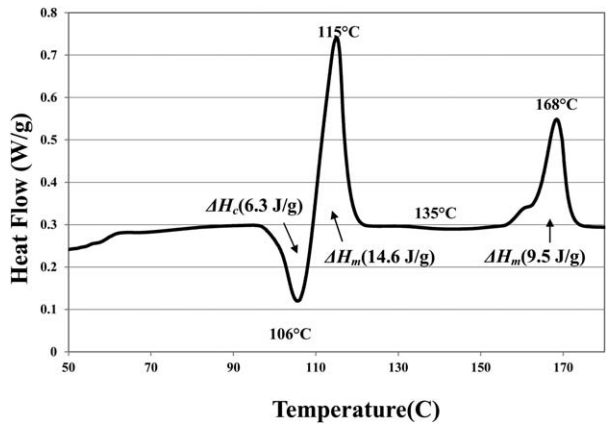

Figure 6. Second heating run for ternary blend of 33%PBS/33%PLA/33%PBAT.

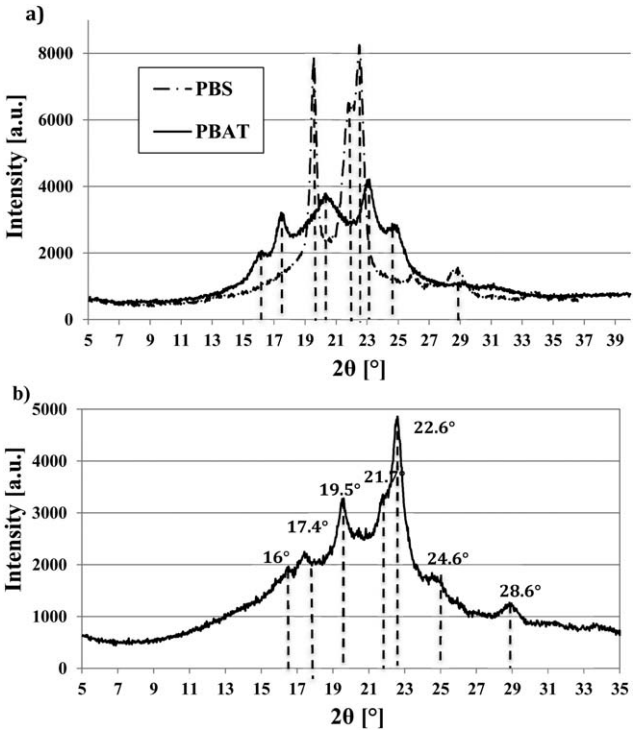

Figure 7. WAXD diffractograms of a) pure PBS, PBAT, and b) ternary blend of 33%PBS/33%PLA/33%PBAT.

The ternary blend of 33%PBS/33%PLA/33%PBAT demonstrates a very high level of properties including a high elongation at break (567%), high Young's modulus (1130 MPa) and high impact strength (271 J/m). Moreover, the storage modulus of this blend increases by 50% at environmental temperatures as compared to neat PBS. The continuity of the components allows them to better contribute to the final properties since the property sets obtained in the final mixture can be more effectively shared from the three different polymers.

An optimized toughness and tensile strength are strongly dependent on the level of crystallinity with semicrystalline structures generally preferred. The DSC experiments demonstrate that the PLA phase acts as nucleating agent for the other phases and also the crystallinity of the blend has been modulated through the blending process to a value of 17%. Typical WAXD of the ternary 33%PBS/33%PLA/33%PBAT system confirms that the PBS and PBAT crystal structure remains constant after blending.

These results indicate the significant potential to synergistically tailor properties when using a highly interacting three-phase system where all components are fully continuous.

Acknowledgments

The authors express appreciation to the Natural Sciences and Engineering Research Council of Canada (NSERC) and the Network for Innovative Plastic Materials and Manufacturing Processes (NIPMMP) for supporting this work. The

authors would like to thank Dr. Pierre Sarazin of Cerestech Inc. for interesting discussions and Mr. J.P. Masse for assistance with the XRD results.

Literature Cited

1. Kijchavengkul T, Auras R. Compostability of polymers. *Polymer Int*. 2008;57:793–804.
2. Shibata M, Inoue Y, Miyoshi M. Mechanical properties, morphology, and crystallization behavior of blends of poly(L-lactide) with poly(butylene succinate-co-L-lactate) and poly(butylene succinate). *Polymer*. 2006;47:3557–3564.
3. Ichikawa Y, Mizukoshi T. Bionolle (Polybutylenesuccinate) synthetic biodegradable polymers. In: Rieger B, Künkel A, Coates GW, Reichardt R, Dinjus E, Zevaco TA, editors. *Synthetic Biodegradable Polymers,* Vol. 245. Berlin, Heidelberg: Springer, 2012:285–313.
4. Xu J, Guo B-H. Poly(butylene succinate) and its copolymers: research, development and industrialization. *Biotechnol J*. 2010;5: 1149–1163.
5. Witt U, Einig T, Yamamoto M, Kleeberg I, Deckwer WD, Müller RJ. Biodegradation of aliphatic–aromatic copolyesters: evaluation of the final biodegradability and ecotoxicological impact of degradation intermediates. *Chemosphere*. 2001;44:289–299.
6. Jiang L, Wolcott MP, Zhang J. Study of biodegradable polylactide/poly(butylene adipate-co-terephthalate) blends. *Biomacromolecules*. 2005;7:199–207.
7. Luzinov I, Pagnoulle C, Jerome R. Dependence of phase morphology and mechanical properties of PS/SBR/PE ternary blends on composition: transition from core,Äìshell to triple-phase continuity structures. *Polymer*. 2000;41:3381–3389.
8. Luzinov I, Pagnoulle C, Jerome R. Ternary polymer blend with core-shell dispersed phases: effect of the core-forming polymer on phase morphology and mechanical properties. *Polymer*. 2000;41: 7099–7109.
9. Ravati S, Favis BD. Low percolation threshold conductive device derived from a five-component polymer blend. *Polymer*. 2010;51: 3669–3684.
10. Ravati S, Favis BD. Morphological states for a ternary polymer blend demonstrating complete wetting. *Polymer*. 2010;51:4547–4561.
11. Reignier J, Favis BD. Control of the subinclusion microstructure in HDPE/PS/PMMA ternary blends. *Macromolecules*. 2000;33:6998–7008.
12. Zhang J, Ravati S, Virgilio N, Favis BD. Ultralow percolation thresholds in ternary cocontinuous polymer blends. *Macromolecules*. 2007;40:8817–8820.
13. Torza S, Mason SG. Three-phase interactions in shear and electrical fields. *J Colloid Interface Sci*. 1970;33:67–83.
14. Harkins WD. A general thermodynamic theory of the spreading of liquids to form duplex films and of liquids or solids to form monolayers. *J Chem Phys*. 1941;9:552–568.
15. Friedrich K. Crazes and shear bands in semi-crystalline thermoplastics. In: Kausch HH, editor. *Crazing in Polymers*, Vol. 52–53. Berlin, Heidelberg: Springer, 1983:225–274.
16. Yoshida K, Kawamura T, Terano M, Nitta K-h. Effects of bulk morphology on the mechanical properties of melt-blended PP/PS blends. *J Appl Polym Sci*. 2008;109:211–217.
17. Galeski A. Strength and toughness of crystalline polymer systems. *Prog Polym Sci*. 2003;28:1643–1699.
18. Olf HG, Peterlin A. Cryogenic crazing of crystalline, isotactic polypropylene. *J Colloid Interface Sci*. 1974;47:628–635.
19. Galeski A, Argon AS, Cohen RE. Changes in the morphology of bulk spherulitic nylon 6 due to plastic deformation. *Macromolecules*. 1988;21:2761–2770.
20. Benninghoven A. Chemical analysis of inorganic and organic surfaces and thin films by static time-of-flight secondary ion mass spectrometry (TOF-SIMS). *Angew Chem Int Ed English*. 1994;33:1023–1043.
21. Cox WP, Merz EH. Correlation of dynamic and steady flow viscosities. *J Polym Sci*. 1958;28:619–622.
22. Veenstra H, Verkooijen PCJ, van Lent BJJ, van Dam J, de Boer AP, Nijhof APHJ. On the mechanical properties of co-continuous polymer blends: experimental and modelling. *Polymer*. 2000;41:1817–1826.
23. Paul D, Newman S. *Polymer Blends*. New York: Academic Press, 1978.
24. Jordhamo GM, Manson JA, Sperling LH. Phase continuity and inversion in polymer blends and simultaneous interpenetrating networks. *Polym Eng Sci*. 1986;26:517–524.
25. Ravati S, Favis BD. Tunable morphologies for ternary blends with poly(butylene succinate): partial and complete wetting phenomena. *Polymer*. 2013;54:3271–3281.
26. Utracki LA. *Polymer Blends Handbook*, Vol. 2. Dordrecht, London: Kluwer Academic Publishers, 2002.
27. Yee AF. Mechanical properties of mixtures of two compatible polymers. *Polym Eng Sci*. 1977;17:213–219.
28. Semba T, Kitagawa K, Ishiaku US, Hamada H. The effect of crosslinking on the mechanical properties of polylactic acid/polycaprolactone blends. *J Appl Polym Sci*. 2006;101:1816–1825.
29. Herrera R, Franco L, Rodriguez-Galan A, Puiggali J. Characterization and degradation behavior of poly(butylene adipate-co-terephthalate)s. *J Polym Sci Part A: Polym Chem*. 2002;40:4141–4157.
30. Yoo ES, Im SS. Melting behavior of poly(butylene succinate) during heating scan by DSC. *J Polym Sci Part B: Polym Phys*. 1999;37: 1357–1366.
31. Ihn KJ, Yoo ES, Im SS. Structure and morphology of poly(tetramethylene succinate) crystals. *Macromolecules*. 1995;28:2460–2464.
32. De Santis P, Kovacs AJ. Molecular conformation of poly(S-lactic acid). *Biopolymers*. 1968;6:299–306.
33. Solarski S, Ferreira M, Devaux E. Characterization of the thermal properties of PLA fibers by modulated differential scanning calorimetry. *Polymer*. 2005;46:11187–11192.
34. Yeh J-T, Tsou C-H, Huang C-Y, Chen K-N, Wu C-S, Chai W-L. Compatible and crystallization properties of poly(lactic acid)/poly(-butylene adipate-co-terephthalate) blends. *J Appl Polym Sci*. 2010; 116:680–687.
35. Kuwabara K, Gan Z, Nakamura T, Abe H, Doi Y. Crystalline/amorphous phase structure and molecular mobility of biodegradable poly(butylene adipate-co-butylene terephthalate) and related polyesters. *Biomacromolecules*. 2002;3:390–396.

Manuscript received Jan. 30, 2014, and revision received Apr. 15, 2014.